American Mineralogist, Volume 88, pages 1084–1090, 2003

The crystal chemistry of julgoldite-Fe^{3+} from Bombay, India, studied using synchrotron X-ray powder diffraction and ^{57}Fe Mössbauer spectroscopy

G. ARTIOLI,[1,*] C.A. GEIGER,[2] AND M. DAPIAGGI[1]

[1]Dipartimento di Scienze della Terra, Università di Milano, I-20133 Milano, Italy
[2]Institut für Geowissenschaften, Christian-Albrechts-Universität, D-24098 Kiel, Germany

ABSTRACT

The crystal structure of julgoldite-Fe^{3+} from Bombay, India, was investigated by ^{57}Fe Mössbauer spectroscopy and synchrotron X-ray powder diffraction. Only ferric iron was detected in the Mössbauer measurements and it occurs at two different octahedral sites in the atomic ratio 20:80. Based on Rietveld refinements, the Fe^{3+} cations are located at the X- and Y-octahedral sites with atomic percentages of about 25% and 75%, respectively. The resulting chemical formula of the Bombay julgoldite sample is $Ca_8(Fe^{3+}_{2.7}Al_{1.1}Mg_{0.2})(Fe^{3+}_{8.0})Si_{12}O_{42}(OH)_{14}$. The oxidation state of Fe is not the same as that arrived at through simple crystal-chemical considerations. Such analysis cannot give quantitative results for the valence state of mixed-valence cations in pumpellyite-type minerals and their intracrystalline partitioning behavior. Assignments of the Mössbauer absorption doublets and an analysis of Fe-intracrystalline partitioning behavior are discussed with reference to previous works on different pumpellyite-type minerals.

INTRODUCTION

Pumpellyite-type minerals are mixed group silicates containing isolated SiO_4 tetrahedra and disilicate $Si_2O_6(OH)$ groups. The general formula is given as $W_8X_4Y_8Z_{12}O_{56-n}(OH)_n$, where W is a seven-coordinated site mostly occupied by Ca, X, and Y are two crystallographically independent octahedral sites occupied by divalent and trivalent cations, and Z is a tetrahedral site mostly containing Si (Passaglia and Gottardi 1973). End-members of the pumpellyite-type mineral group are julgoldite (Moore 1971; Allmann and Donnay 1973), shuiskite (Ivanov et al. 1981), okhotskite (Togari and Akasaka 1987; Akasaka et al. 1997), and V-pumpellyite (Pan and Fleet 1992). The name pumpellyite, julgoldite, shuiskite, or okhotskite depends on whether Al, Fe, Cr, or Mn is the prevailing cation at the Y-site. A suffix should be added to indicate the major cation at the X-site (Passaglia and Gottardi 1973). The structures and crystal chemistries of pumpellyite-type minerals are closely related to those of several silicate minerals containing disilicate (e.g., sursassite, macfallite) or trisilicate groups (e.g., ardennite, orientite) and to synthetic Ca-free high-pressure phases (Schreyer et al. 1986; Schreyer et al. 1987; Artioli et al. 1999; Gottschalk et al. 2000).

Although the basic crystal structures of pumpellyite-Al and julgoldite-Fe have long been known (Gottardi 1965; Galli and Alberti 1969; Allmann and Donnay 1973; Yoshiasa and Matsumoto 1985), the crystal-chemical role of multi-valence elements (i.e., Fe and Mn) has only recently been investigated (Artioli and Geiger 1994; Artioli et al. 1996; Akasaka et al. 1997). Iron, in particular, has been studied using X-ray powder diffraction methods (Artioli and Geiger 1994), X-ray absorption spectroscopy (XAS: Artioli et al. 1991) and ^{57}Fe Mössbauer spectroscopy (MS: Artioli and Geiger 1994; Akasaka et al. 1997). XAS proved to be unsuitable for determining the valence state of Fe and its intracrystalline partitioning. Mössbauer spectroscopy, on the other hand, has proven better in this regard. All previous crystal-chemical studies were performed on Fe-rich pumpellyite samples, and they gave different partitioning schemes for Fe^{2+} and Fe^{3+} over the X- and Y-sites. Artioli and Geiger (1994), based on a complementary powder diffraction and Mössbauer spectroscopy study of Fe-rich pumpellyite-Al samples from Keweenawan, Michigan, and Bulla, Italy, proposed that divalent and trivalent iron cations are partitioned in the X- and Y-octahedral sites, respectively. Akasaka et al. (1997), based on a Mössbauer spectroscopy study of pumpellyite-Fe samples from Tokoro and Mitsu, Japan, concluded that Fe^{2+} can also occur at the seven coordinated W-site, and that the X-site may host Fe^{2+} and Fe^{3+} in different proportions.

No Mössbauer spectroscopic measurements have been made on true julgoldite, that is on samples having Fe as the prevalent cation on the Y-site, or on samples having a total iron content larger than six octahedral cations per unit cell. The present study, therefore, contributes to ongoing investigations concerning the valence state and Fe intracrystalline behavior in pumpellyite-type structures using synchrotron X-ray powder diffraction (XRPD) and ^{57}Fe Mössbauer spectroscopy (MS).

EXPERIMENTAL METHODS

Samples

To date, julgoldite has been reported from Långban, Sweden (Moore 1971), Noril'sk, Russia (Zolotukhin et al. 1965), Ratho and Auchinstarry, Scotland (Livingstone 1976), and Bombay, India (Ottens 2001; Wise and Moller 1990). We tried to obtain samples from each of these localities, either from the original authors reporting the occurrences, or from museums and dealers. The amount of samples from Långban and Scotland that were made available to us were much too scarce for study either by XRPD or MS. The only samples containing julgoldite in some quantity were those from the quarries near Bombay, India.

* E-mail: artioli@iummix.terra.unimi.it

Here, the crystals occur as dark brown, fine needle-like aggregates together with ilvaite, hematite, chlorite, quartz, and other Ca silicate minerals, such as prehnite and laumontite. The julgoldite habit and mineral association are very similar to that reported by Ottens (2001) and Wise and Moller (1990) for their pumpellyite-Fe^{2+} samples. Two julgoldite separates, labeled JULG-A and JULG-B, were obtained by hand picking, under a microscope the fine needles from two different hand specimens from the same locality. The purity of the separates was checked by laboratory XRPD. Sample JULG-A consists of pure julgoldite, whereas JULG-B shows about 1.4 wt% quartz as determined from multiphase Rietveld refinement. The small size of the needles, which are composed of multiple crystals, precluded analysis by single crystal diffraction methods.

Quantitative chemical analyses of hand-separated crystals were performed using an Applied Research Laboratories electron microprobe fitted with six wavelength-dispersive spectrometers. The system was operated using a defocused electron beam at an accelerating voltage of 15 kV and a sample current determined on brass of 15 nA. A series of natural minerals were employed as standards. The results were corrected for matrix effects using a conventional ZAF routine in the Tracor Northern TASK series of programs. The results averaged from six point analyses are listed in Table 1.

Both samples were finely ground in an agate mortar and inserted in capillaries for the synchrotron XRPD data collection. One of the samples (JULG-A) was investigated by MS.

Mössbauer spectroscopy measurements

The Mössbauer spectrum was collected at room temperature using a nominal 1.85 GBq ^{57}Co/Rh source. Julgoldite powder was mixed together with corn starch and pressed into a pellet of diameter 12 mm to give approximately 5 mg Fe^{2+}/cm^2. Mirror-image spectra were collected in both 90° and 54°44' geometries to test for preferred orientation effects using a 1024 multichannel analyzer, and were then folded. Spectra were obtained from Fe-metal foil for calibration. The spectra were fit with the least-squares fitting program MÖSALZ (courtesy of W. Lottermoser, Salzburg University) using Lorentzian doublets with equal areas for the high- and low-velocity peaks. It was deemed unnecessary to record spectra at 77 K, because published results do not indicate major changes upon cooling for Fe^{3+}-rich samples (Artioli and Geiger 1994).

Synchrotron X-ray powder data collection

Powder diffraction data were collected at the BM16 beamline at the European Synchrotron Radiation Facility (ESRF), Grenoble, France. The bending magnet beamline optics encompasses a double-crystal Si(311) monochromator and vertically focusing optics. Technical details of the beamline can be found on the ESRF web page at http://www.esrf.fr. A wavelength of 0.710127(2) Å was selected for the experiment and calibrated against elemental silicon (NBS 640b, having a = 5.430954 Å at 26 °C). The two julgoldite samples, composed of extremely fine needles, were crushed in an agate mortar, loaded into 0.3 mm diameter Lindemann capillaries and attached to a standard goniometer head. The latter was mounted on the ϕ axis of the two-circle diffractometer and was axially rotated during the data collection in Debye-Scherrer geometry. Diffraction patterns were collected using the standard nine channel detector available at BM16, where each detector was equipped with a Ge analyzer crystal. The signals accumulated by the detectors were then merged and corrected for the incident beam variation in time using locally written software. The final measured angular range is 2.0–56.0° 2θ. The step size of the rebinned histograms is 0.02° 2θ.

The subsequent structure analysis was performed by the full-profile Rietveld method using GSAS software (Larson and Von Dreele 1998).

TABLE 1. Electron probe microanalyses of julgoldite from Bombay, India

Oxide	wt%	e.s.d.	element	atoms pfu†
SiO_2	33.58	0.33	Si	12.12
TiO_2	nd		Ti	–
Al_2O_3	1.70	0.27	Al	0.72
Fe_2O_3	39.33	0.60	Fe^{3+}	10.69
CaO	19.13	0.33	Ca	7.40
Mn_2O_3	0.04	0.05	Mn^{3+}	0.01
MgO	0.37	0.03	Mg	0.20
Na_2O	0.06	0.03	Na	0.01
K_2O	nd		K	–
OH^*	5.83		OH	14.04
	100.00			

* By difference.
† Based on 56 O,OH.

RESULTS

Mössbauer fitting

The Mössbauer spectrum is shown in Figure 1 and the fit parameters are listed in Table 2. Isomer shifts (IS) are relative to α-iron and the estimated errors in the IS and quadrupole splitting (QS) are about 0.02 mm/s. No texture effects were observed. The spectrum indicates that all iron in the Bombay julgoldite is trivalent, and that it is located at octahedral sites. The spectrum can be fit with two different models. The first is based on two doublets. The assignment of the two doublets to Fe^{3+} at the Y- and X-sites is based on their IS values (i.e., 0.35–0.40 mm/s) and the known crystal structure of julgoldite. The second model uses three doublets, where a third weak doublet with IS = 0.38 mm/s, QS = 0.71 mm/s, and an intensity of 4% is included. Such a fit is difficult to interpret crystal chemically. Therefore, we adopt herein the two-doublet model, while recognizing that Fe^{3+} in small amounts could be located at another site or possibly in another phase.

Rietveld refinement analysis

The starting structural model for julgoldite, space group *A2/m*, was taken from Allmann and Donnay (1973), who reported refined structure and atomic coordinates very similar to those cited for pumpellyite (Galli and Alberti 1969; Yoshiasa and Matsumoto 1985). The starting composition was based on the chemical analysis (Table 1). The W and Z sites were constrained to be fully occupied by Ca and Si, respectively, in agreement with the reported analysis. The electron density of the X-

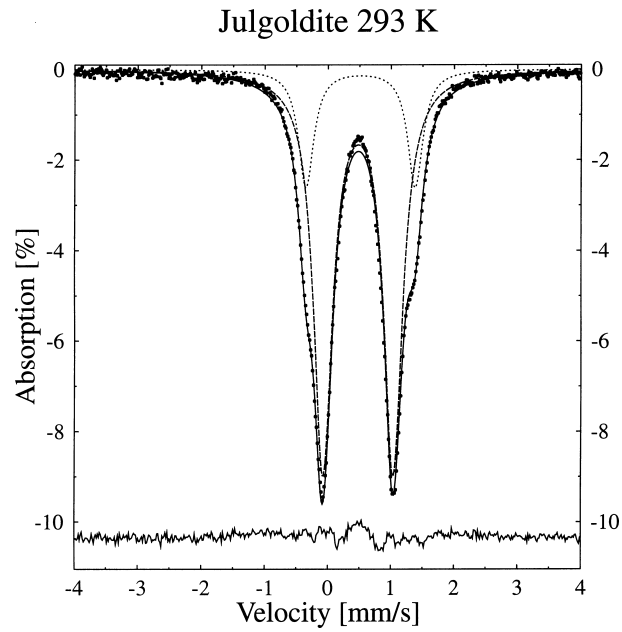

FIGURE 1. ^{57}Fe Mössbauer spectrum of julgoldite (sample JULG-A) showing a two doublet fit. The fit parameters are listed in Table 2.

and Y-octahedral sites was modeled with a mixed occupancy of Al and Fe, assuming full site occupancy and a starting ratio of 50% Al and 50% Fe for each site, to avoid biasing the site occupancies. This composition corresponds to an iron-poor julgoldite with six Fe atoms and six Al atoms per unit cell that plots between the julgoldite and pumpellyite compositional fields. The Mg content of the octahedral sites is almost negligible (Table 1) and furthermore X-ray powder data can hardly discriminate between Al^{3+} and Mg^{2+} because they are iso-electronic. The X- and Y-sites were therefore modeled using Al and Fe alone, although a small proportion of the Al is actually Mg. It is probably located at the X-site as shown by all previous structure studies of pumpellyite-type minerals.

The basic structure model was initially kept fixed to extract reasonable peak-profile parameters, a background-modeling curve, and unit-cell parameters for both julgoldite samples. The first Rietveld fits showed: (1) the presence of quartz as an impurity phase in sample JULG-B (therefore quartz was inserted as a second phase in the refinement) and (2) that both samples have the same cell parameters within uncertainty. Because all previous studies showed that the cell volume is proportional to the total Fe content (Passaglia and Gottardi 1973; Artioli and Geiger 1994; Akasaka et al. 1997), the two samples ought to have the same composition. Preliminary unconstrained refinement of the Fe contents at the two octahedral sites indicated a total atomic iron content close to 10 per unit cell for both samples, and a full iron occupancy of the Y site.

After these initial steps, a simultaneous multiphase Rietveld refinement was performed, using both data sets to obtain a unique structure model. This strategy, employing redundant data, confers stability and better convergence to the least-squares minimization procedure. In the final cycles the following parameters were refined: one scale factor for each histogram and for each phase, three coefficients for the polynomial background function and the zero-shift correction for each histogram, two coefficients of the Lorentzian part of the pseudo-Voigt function describing the peak profiles, the unit-cell parameters of julgoldite and quartz, the atomic coordinates and the isotropic displacement parameters of all atoms in julgoldite and the site-occupancy factors for the octahedral sites. The scattering power at the X octahedral sites was refined assuming full site occupancy, i.e., Al(X) + Fe(X) = 1, whereas the Y-site consistently showed full iron occupancy and was fixed in the last cycles. Correction for preferred orientation using a cylindrical sample and a fiber-axis model was attempted by spherical harmonics of order 4. The resulting texture index was 1.039, indicating very limited preferred orientation of the julgoldite needles parallel to the capillary axis.

A summary of the Rietveld refinement parameters is given in Table 3. Structural parameters are listed in Table 4 and interatomic distances and angles are listed in Table 5. Figure 2 shows the final observed, calculated, and difference powder diffraction patterns for JULG-A. The JULG-B patterns are nearly identical and were therefore omitted, but they are available from the authors on request.

TABLE 2. ^{57}Fe Mössbauer parameters for the JULG-A sample and pumpellyite form Bulla, Italy

Sample	Temperature	Doublets	IS*	QS	FWHH	Absorption %
				(mm/s)	(mm/s)	(mm/s)
julgoldite	293 K	Fe^{3+} doublets	0.40	1.73	0.30	20
			0.36	1.11	0.36	80
pumpellyite	77 K	Fe^{3+} doublets	0.41	2.00	0.28	4
			0.42	1.16	0.42	74
		Fe^{2+} doublets	1.36	2.72	0.33	9
			1.24	3.46	0.35	13
	293 K	Fe^{3+} doublets	0.42	1.70	0.28	5
			0.34	1.14	0.38	73
		Fe^{2+} doublets	1.20	2.56	0.35	8
			1.09	3.33	0.28	14

* Relative to Fe metal.

DISCUSSION

Crystal chemistry

The structure of the Bombay sample is similar to that reported for the Långban material (Allmann and Donnay 1973). The mean cation-O atom bond distances (Table 5) differ from those of the Långban sample only by about 0.01 Å for all coordination polyhedra. An exception is the Y-octahedron, where the mean (Al,Fe)-O distance in the Bombay julgoldite is 2.05 Å, compared to a mean distance of 2.01 Å in the Långban sample. This might be due to small differences in their compositions and cation partitioning state. The Långban julgoldite is

TABLE 3. Results of the Rietveld refinement of the Bombay julgoldite

Space group	*A*2/*m*		
a (Å)	8.8879(4)		
b	6.0580(2)		
c	19.3321(7)		
β (°)	97.498(2)		
Cell volume (Å^3)	1032.01(7)		
	Combined	Histogram A	Histogram B
Angular range (°2θ)		3.5–56.0	3.5–56.0
No. data points in histogram		10499	10499
$R_{wp} = [\Sigma w(I_o - I_c)^2/\Sigma w I_o^2]^{1/2}$	0.2251	0.2253	0.2252
$\chi^2 = \Sigma w(I_o - I_c)^2/N_{obs} - N_{var}$	0.9905		
$R_{F2} = \Sigma\lvert F_o^2 - F_c^2\rvert/\Sigma\lvert F_o^2\rvert$		0.1779	0.1553
No. Bragg reflections		1549	1549
No. refined parameters	73		

TABLE 4. Refined atomic coordinates for the Bombay julgoldite sample

Atom	*x*	*y*	*z*	U_{iso}	Occ.
Si1	0.049(1)	0	0.0977(6)	0.006(1)	1.0
Si2	0.168(1)	0	0.2479(7)	0.006(1)	1.0
Si3	0.468(2)	0	0.4040(6)	0.006(1)	1.0
O1	0.132(1)	0.233(2)	0.0793(7)	0.013(1)	1.0
O2	0.269(1)	0.224(2)	0.2458(8)	0.013(1)	1.0
O3	0.370(1)	0.228(2)	0.4102(6)	0.013(1)	1.0
O4	0.123(2)	1/2	0.443(1)	0.013(1)	1.0
OH5	0.116(2)	0	0.452(1)	0.013(1)	1.0
O6	0.373(2)	1/2	0.043(1)	0.013(1)	1.0
OH7	0.388(2)	0	0.035(1)	0.013(1)	1.0
O8	0.038(2)	0	0.1811(6)	0.013(1)	1.0
O9	0.464(2)	1/2	0.1718(8)	0.013(1)	1.0
OH10	0.070(2)	0	0.3138(9)	0.013(1)	1.0
OH11	0.509(2)	1/2	0.322(1)	0.013(1)	1.0
Ca1	0.258(1)	1/2	0.3392(4)	0.017(1)	1.0
Ca2	0.1819(9)	1/2	0.1534(4)	0.017(1)	1.0
X-Al	1/2	1/4	1/4	0.012(1)	0.312(8)
X-Fe	1/2	1/4	1/4	0.012(1)	0.688(8)
Y-Al	0.2532(5)	0.250(1)	0.4956(2)	0.012(1)	0.0
Y-Fe	0.2532(5)	0.250(1)	0.4956(2)	0.012(1)	1.0

TABLE 5. Selected inter-atomic distances (Å) and angles (°) for the Bombay julgoldite sample

X-O2	×2	2.05(1)	Si1-O1	×2	1.651(6)
X-O9	×2	2.13(1)	Si1-O4		1.627(8)
X-OH11	×2	2.05(1)	Si1-O8		1.629(8)
mean		2.08	mean		1.640
			Si2-O2	×2	1.634(5)
Y-O1		2.06(1)	Si2-O8		1.615(8)
Y-O3		2.07(1)	Si2-OH10		1.632(8)
Y-O4		2.09(1)	mean		1.629
Y-OH5		2.05(2)	Si3-O3	×2	1.646(6)
Y-O6		2.00(1)	Si3-O6		1.632(8)
Y-OH7		2.02(2)	Si3-O9		1.653(8)
mean		2.05	mean		1.644
Ca1-O2	×2	2.47(1)	Ca2-O1	×2	2.17(1)
Ca1-O3	×2	2.29(1)	Ca2-O2	×2	2.49(2)
Ca1-O4		2.48(2)	Ca2-O6		2.90(2)
Ca1-O8		2.61(2)	Ca2-O9		2.49(2)
Ca1-OH11		2.29(2)	Ca2-OH10		2.41(2)
mean		2.41	mean		2.45
O1-Si1-O1		117.6(9)			
O1-Si1-O4	×2	108.0(8)			
O1-Si1-O8	×2	107.5(8)			
O4-Si1-O8		107.8(9)			

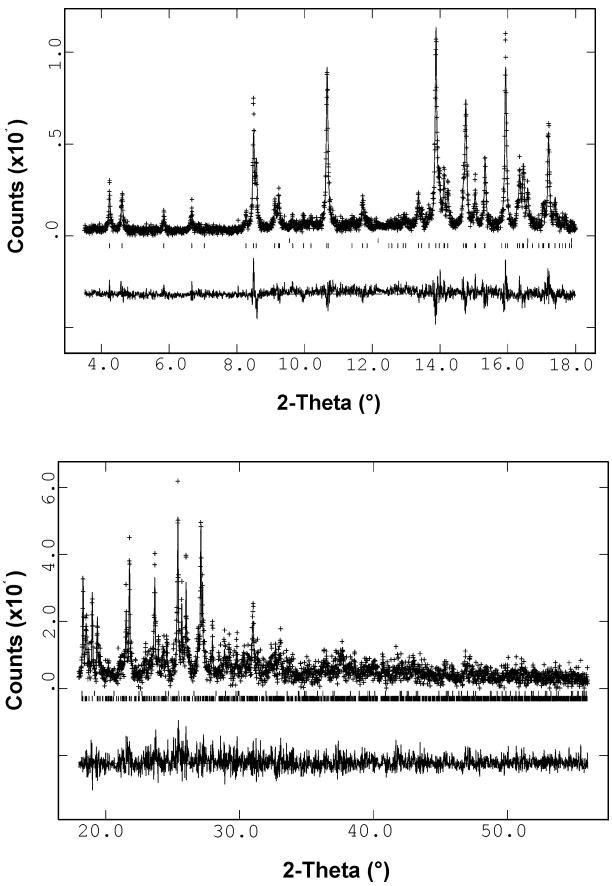

FIGURE 2. Observed (crosses), calculated (continuous upper line), and difference (continuous lower line) powder diffraction patterns for the Rietveld refinement of the JULG-A julgoldite sample.

reported to have nearly 12 Fe atoms per cell, whereas the total Fe content of the Bombay sample is about 10.8 atoms per cell (Table 1). The polyhedral distortion indices for the Bombay julgoldite for the X- and Y-sites are shown in Table 6 and are compared with those calculated from literature data (Artioli and Geiger 1994; Galli and Alberti 1969; Allmann and Donnay 1973). In julgoldite, and other pumpellyites as well, the Y-site is more distorted than the X-site, although the QE values of the two sites are similar and show small deviations from an ideal octahedron.

The refinement-based iron content is in very good agreement with that determined by chemical analysis (10.7 atoms per cell, Table 1), and with that determined from the total Fe content vs. cell-volume relationship for the pumpellyite-julgoldite series (Fig. 3). In Figure 3 all reliable unit-cell determinations for this solid solution, as taken from the literature, are shown together with the oxidation state of Fe determined from structural and spectroscopic results. The relationship between Fe content and cell volume (Passaglia and Gottardi 1973; Artioli and Geiger 1994; Akasaka et al. 1997) is confirmed. The presence of Fe^{2+} does not greatly affect the cell volume, whereas the smaller and more highly charged Fe^{3+} cations generates octahedral distortion in the crystal structure (Fig. 3). Figure 4a shows the variation in unit-cell values as a function of the total Fe content. Figure 4b shows the unit-cell values in each crystallographic direction normalized to the number of octahedra contributing to the change.

The structure of pumpellyite and julgoldite may be described as consisting of chains of edge-sharing octahedra (i.e., X-chains and Y-chains) linked by SiO_4, Si_2O_7, and CaO_7 polyhedra (Gottardi 1965; Galli and Alberti 1969; Allmann and Donnay 1973; Yoshiasa and Matsumoto 1985). The X- and Y-chains are parallel to the [010] crystallographic direction, and, therefore, two edge-sharing octahedra cause variations in the *b* cell parameter. Two layers of X-chains and one layer of Y-chains occur along the [100] direction, whereas two layers of both X-chains and Y-chains occur along the [001] direction. Therefore, three- and four-linked octahedra are responsible for changes in the *a* and *c* cell parameters, respectively. It is interesting to note that the contribution of Fe^{3+} to the change in the different cell parameters does not appear to be affected by its partitioning behavior between the two octahedral sites. The anisotropic distortion of pumpellyite-type structures is largely independent of the intracrystalline partitioning behavior of iron.

TABLE 6. Polyhedral distortion indices for the Bombay julgoldite as compared to those of previously refined pumpellyite structures

Mineral	X site		Y site	
	QE	AV	QE	AV
Bombay julgoldite	1.0024	5.9807	1.0048	16.294
Hicks Ranch, California*	1.0055	18.201	1.0090	28.390
Keweenawan, Michigan*	1.0095	26.645	1.0104	34.007
Torrente Bulla, Italy*	1.0076	19.789	1.0092	30.157
Hicks Ranch, California†	1.0057	16.091	1.0101	33.522
Langban, Sweden‡	1.0062	14.549	1.0089	29.586

Notes: QE = quadratic elongation, AV = angle variance; see Robinson et al. 1971 for definitions.
* Artioli and Geiger 1994.
† Galli and Alberti 1969.
‡ Allmann and Donnay 1973.

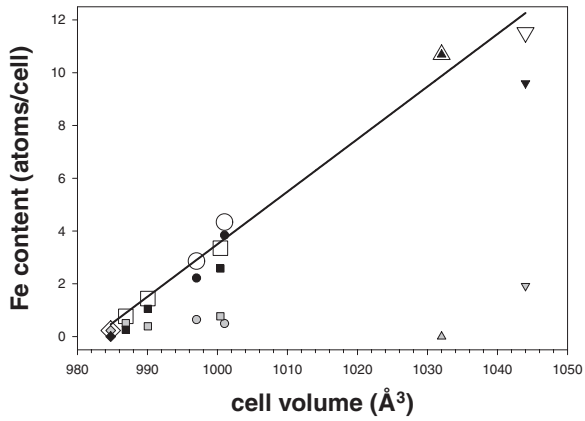

FIGURE 3. Atomic Fe content vs. unit-cell volume for the pumpellyite-julgoldite series. Large open symbols refer to the total atomic Fe content, small black symbols to the Fe^{3+} content, and small gray symbols to the Fe^{2+} content, in atoms per unit cell. Data are as follows: diamonds (Yoshiasa and Matsumoto 1985), squares (Artioli and Geiger 1994), circles (Akasaka et al. 1997), downward triangles (Allmann and Donnay 1973), upward triangles (present study).

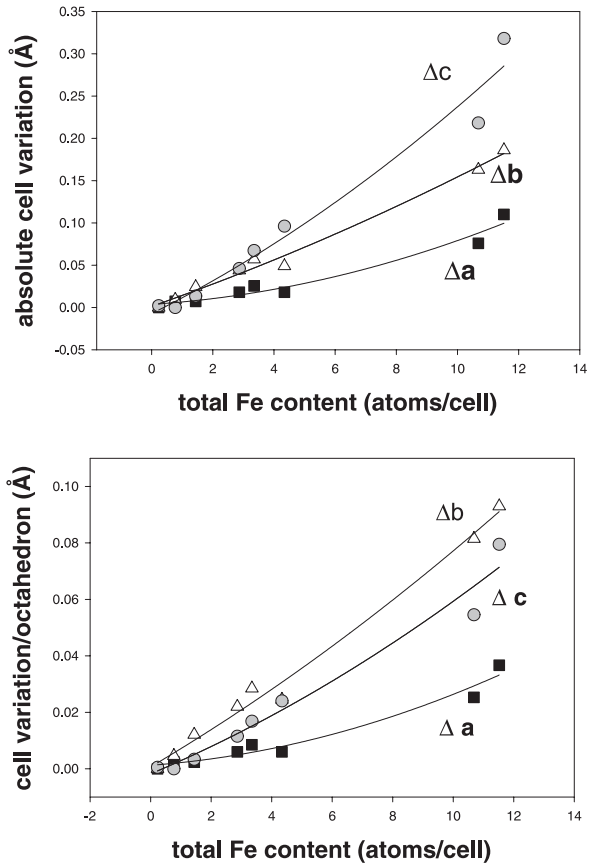

FIGURE 4. (**a**) Variation of the unit-cell parameters as a function of the total Fe content in pumpellyite and julgoldite minerals. (**b**) Variation in the unit-cell parameters as a function of the total Fe content normalized against the number of octahedral sites in each crystallographic direction. Sources of data are as in Figure 3.

Intracrystalline Fe partitioning

There is uncertainty with regard to interpretation of the ^{57}Fe Mössbauer spectra and the intracrystalline partitioning behavior of Fe in pumpellyite-type minerals, and different models have been proposed (Artioli and Geiger 1994; Artioli et al. 1996; Akasaka et al. 1997). The task is not simple for several reasons. Fe-rich samples rarely produce good large crystals and previous single-crystal diffraction studies, which made elemental site-fraction determinations, were done with Fe-poor crystals. There are contradicting interpretations of Fe-site occupancy behavior based on powder X-ray refinements vs. those determined from Mössbauer spectroscopy. Precise single-crystal X-ray results would be best for interpreting the spectroscopic measurements. In addition, Mössbauer spectra measured on samples containing both Fe^{2+} and Fe^{3+} are difficult to interpret because of the strong overlap of the different low-velocity Fe^{3+} and Fe^{2+} absorption lines. The problem is further compounded because pumpellyite-type minerals can contain Fe (and Mn) in two different valence states, and the multivalent cations can theoretically be located at three (or more) different structural sites. It is also probable that pumpellyite is characterized by some nonstoichiometry.

It is possible now, however, to reconsider the various data and different previous interpretations, because our julgoldite sample has a simple Fe-intracrystalline partitioning behavior. Thus, it can be used as a starting or anchor point for analyzing other pumpellyite samples. Our spectrum of julgoldite is comparable in appearance to the okhotskite sample of Akasaka et al. (1997) and can be fit similarly with two Fe^{3+} doublets. Adopting the octahedral Fe partitioning state determined from the Rietveld refinement on julgoldite, we assign in the Mössbauer spectrum the weaker doublet with the larger QS of 1.73 mm/s to Fe^{3+} at the X-octahedral site and the more intense doublet with QS = 1.11 mm/s to Fe^{3+} at the Y site. The spectrum gives an atomic Fe^{3+} X-site:Y-site ratio of 20:80. This agrees well with the site occupancy ratio of 25:75 from the Rietveld refinement (Table 4). In our earlier works on pumpellyite minerals, following the proposal of Passaglia and Gottardi (1973) that the Y-site contains the smaller cations, it was suggested that Fe^{3+} is located exclusively at the smaller Y-site. This interpretation is incorrect, as pointed out by Akasaka et al. (1997). Their Mössbauer spectrum of pumpellyite-Al was fit with four QS doublets and they proposed that Fe^{3+} occurs at both X- and Y-sites with the majority, however, located at the X-site. If our Rietveld refinement is accurately reflecting the Fe-partitioning behavior, then our Fe^{3+} doublet assignments should be correct.

The next question concerns the Fe^{2+} intracrystalline partitioning behavior in pumpellyite. Fe^{2+} can, theoretically, be located at the W-, X- and Y-sites. Artioli and Geiger (1994) fitted two Fe^{2+} QS doublets to the spectrum of a ferrous-rich pumpellyite from Hicks Ranch, California. They suggested that Fe^{2+} was located at the X-site exclusively and that the two or more doublet fit resulted from X-sites having slightly different distortions arising from the presence or absence of OH groups. We retract this proposal and suggest, instead, that as with Fe^{3+}, a two-doublet fit best explains the data and that they are related to Fe^{2+} occurring at the X- and Y-sites. This is the sim-

plest and most logical interpretation. Akasaka et al. (1997) proposed a partitioning scheme in which Fe^{2+} could be located at the W- and X-sites. They assigned a Fe^{2+} doublet with an IS = 0.97 mm/s to the X-site of their Tokoro pumpellyite-Al sample and a second Fe^{2+} doublet with an IS = 1.01 mm/s to Fe^{2+} at the sevenfold coordinated W-site and recognized that these values are not entirely consonant with known IS systematics for Fe^{2+}. The IS value of 0.97 mm/s does not fall in the range of octahedral Fe^{2+} observed in various silicates (1.07–1.25 mm/s; McCammon 2000) and the IS for the sevenfold W-site is also rather low for this coordination (based on IS systematics it should be around 1.2–1.3 mm/s). Their results show, furthermore, variations in the hyperfine parameters and line widths for the same assigned doublet in the different samples they studied. This suggests some uncertainty in their fits and doublet assignments.

To better and more completely address the question of Fe-intracrystalline partitioning behavior, we refit the Mössbauer spectrum of the most Fe^{3+}-rich pumpellyite sample studied by Artioli and Geiger (1994) from Bulla, Italy. Figure 5 shows the spectrum recorded at 77 K and 298 K. A fit was made using two Fe^{3+} and two Fe^{2+} doublets. The starting positions of the Fe^{3+} doublets were chosen to give hyperfine parameters similar to those of the julgoldite sample, and then two Fe^{2+} doublets were added in the least-squares procedure. The final best-fit results (Table 2) show good agreement in the hyperfine parameters for Fe^{3+} for the Bulla sample and the Bombay julgoldite. The hyperfine parameters for the two Fe^{2+} doublets are also reasonable for Fe^{2+} in octahedral coordination. Fe^{2+} appears to be more strongly partitioned into the X-site.

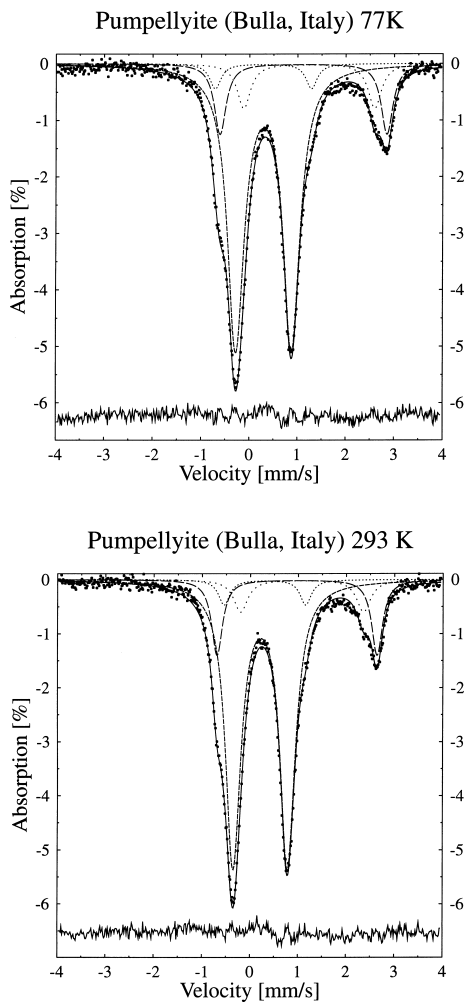

FIGURE 5. ^{57}Fe Mössbauer spectrum of pumpellyite from Bulla, Italy at 77 K (**a**) and 298 K (**b**) showing a four doublet fit. The fit parameters are listed in Table 1.

The present results show that caution should be exerted when assigning Mössbauer doublets on the basis of the hyperfine parameters (Ingalls 1964; Rancourt 1998). Results for the Fe^{2+} and the Fe^{3+} partitioning behavior contradict the idea that cation radii, site size, and site distortion alone govern the site partitioning in pumpellyite minerals (Passaglia and Gottardi 1973). Fe^{2+} will gain a greater crystal field stabilization energy by being in the smaller X-site compared to the Y-site and such energetic contributions must also be considered in any quantitative site-partitioning model. It should be noted that the present Mössbauer spectra continue to show a small amount of misfit. Some of this may be explained by local compositional heterogeneity around the X- and Y-sites and the use of simple Lorentzians to fit the spectra. Also, further careful study could reveal more information, for example, as to whether Fe can occur in small amounts at other structural sites.

On the basis of the combined X-ray diffraction and Mössbauer tudy, it is shown that Fe only occurs in the ferric state, contrary to what has been postulated on the basis of chemical analyses and purely crystallochemical considerations (Wise and Moller 1990). The combination of the two experimental techniques allows a new interpretation of the intracrystalline distribution of the iron cations over the two crystallographically independent octahedral sites to be proposed. The proposed chemical formula for the Bombay julgoldite is $Ca_8(Fe^{3+}_{2.7}Al_{1.1}Mg_{0.2})(Fe^{3+}_{8.0})Si_{12}O_{42}(OH)_{14}$. Based on the accepted rules for the nomenclature of pumpellyite-type minerals (Passaglia and Gottardi 1973), the Bombay mineral is to be termed julgoldite-Fe^{3+}, because Fe^{3+} cations are dominant in both octahedral sites.

ACKNOWLEDGMENTS

Italian MIUR is acknowledged for funding. A. Fitch is thanked for help during data collection at the BM16 beamline at ESRF. B. Ottens kindly provided the julgoldite samples. U. Russo and M. Grodzicki are thanked for discussion on the interpretation of the Mössbauer data and F. Ferri kindly performed the EPMA analyses. C. McCammon and C. Hoffman provided helpful reviews that improved the manuscript. M. Akasaka read the final draft and also provided useful comments.

REFERENCES CITED

Akasaka, M., Kimura, Y., Omori, Y., Sakakibara, M., Shinno, I., and Togari, K. (1997) ^{57}Fe Mössbauer study of pumpellyite-okhotskite-julgoldite series of minerals. Mineralogy and Petrology, 61, 181–198.

Allmann, R. and Donnay, G. (1973) The crystal structure of julgoldite. Mineralogical Magazine, 39, 271–281.

Artioli, G. and Geiger, C.A. (1994) The crystal chemistry of pumpellyite: an X-ray Rietveld refinement and ^{57}Fe Mössbauer study. Physics and Chemistry of Minerals, 20, 443–453.

Artioli, G., Sacchi, M., Balerna, A., Burattini, E., and Simeoni, S. (1991) XANES

studies of Fe in pumpellyite-group minerals. Neues Jahrbuch Mineralogie Monatshefte, 9, 413–421.
Artioli, G., Pavese, A., Bellotto, M., Collins, S.P., and Lucchetti, G. (1996) Mn crystal chemistry in pumpellyite: a resonant scattering powder diffraction Rietveld study using synchrotron radiation. American Mineralogist, 81, 603–610.
Artioli, G., Fumagalli, P., and Poli, S. (1999) The crystal structure of $Mg_8(Mg_2Al_2)Al_8Si_{12}(O,OH)_{56}$ pumpellyite and its relevance in ultramafic systems at high pressure. American Mineralogist, 84, 1906–1914.
Galli, E. and Alberti, A. (1969) On the crystal structure of pumpellyite. Acta Crystallographica, B25, 2276–2281.
Gottardi, G. (1965) Die Kristallstruktur von Pumpellyit. Tschermaks Mineralogische und Petrographische Mitteilungen, 10, 115–119.
Gottschalk, M., Fockenberg, T., Grevel, K.D., Wunder, B., Wirth, R., Schreyer, W., and Maresch, W.V. (2000) Crystal structure of the high pressure phase $Mg_4(MgAl)Al_4[Si_6O_{21}/(OH)_7]$: an analogue of sursassite. European Journal of Mineralogy, 12, 935–945.
Ingalls, R. (1964) Electric-field gradient tensor in ferrous compounds. Physical Review, 133A, 787–795.
Ivanov, O.K., Arkhangel'skaya, L.O., Miroshinikova, L.O., and Shilova, T.A. (1981) Shuiskite, the chromium analogue of pumpellyite, from the Bisersk deposit. Zapiski Vsesoyuznogo Mineralogicheskogo Obshchestva, 110, 508–512.
Larson, A.C. and Von Dreele, R.B. (1998) GSAS General Structure Analysis System. Report LAUR 86-748. Los Alamos National Laboratory, Los Alamos, New Mexico.
Livingstone, A. (1976) Julgoldite, new data and occurrences: a second recording. Mineralogical Magazine, 40, 761–763.
McCammon, C.A. (2000) Insights into phase transformations from Mössbauer spectroscopy. In S.A.T. Redfern and M.A. Carpenter, Eds., Transformation Processes in Minerals, 39, p. 241–264. Reviews in Mineralogy and Geochemistry, Mineralogical Society of America and The Geochemical Society, Washington, D.C.
Moore, P.B. (1971) Julgoldite, the Fe^{2+}-Fe^{3+} dominant pumpellyite. Lithos, 4, 93–99.
Ottens, B. (2001) Some minerals from Deccan Trapp. Part II. Rivista Mineralogica Italiana, 1, 4–24.
Pan, Y. and Fleet, M.E. (1992) Vanadium-rich minerals of the pumpellyite group from the Hemlo gold deposit, Ontario. Canadian Mineralogist, 30, 153–162.
Passaglia, E. and Gottardi, G. (1973) Crystal chemistry and nomenclature of pumpellyites and julgoldites. Canadian Mineralogist, 12, 219–223.
Rancourt, D.G. (1998) Mössbauer spectroscopy in clay science. Hyperfine Interactions, 117, 3–38.
Robinson, K., Gibbs, G.V., and Ribbe, P.H. (1971) Quadratic elongation: a quantitative measure of distortion in coordination polyhedra. Science, 172, 567–570.
Schreyer, W., Maresch, W.V., Medenbach, O., and Baller, T. (1986). Calcium-free pumpellyite, a new synthetic hydrous Mg-Al-silicate formed at high pressures. Nature, 321, 510–511.
Schreyer, W., Maresch, W.V., and Baller, T. (1987). MgMgAl-pumpellyite: A new hydrous high-pressure, synthetic silicate resulting from Mg-for-Ca substitution. Terra Cognita, 7, 385.
Togari, K. and Akasaka, M. (1987) Okhotskite, a new mineral, an Mn^{3+}-dominant member of the pumpellyite group, from the Kokuriki mine, Hokkaido, Japan. Mineralogical Magazine, 51, 611–614.
Wise, W.S. and Moller, P. (1990) Occurrence of Ca-Fe silicate minerals with zeolites in basalt cavities at Bombay, India. European Journal of Mineralogy, 2, 875–883.
Yoshiasa, A. and Matsumoto, T. (1985) Crystal structure refinement and crystal chemistry of pumpellyite. American Mineralogist, 70, 1011–1019.
Zolotukhin, V.V., Vasil'yev, Yu.R., and Zyuzin, N.I. (1965) Iron rich pumpellyite from the Noril'sk district and a new diagram for pumpellyites. Doklady Akademii Nauk U.S.S.R., Earth Sciences, 165, 136–139.

MANUSCRIPT RECEIVED SEPTEMBER 17, 2002
MANUSCRIPT ACCEPTED FEBRUARY 03, 2003
MANUSCRIPT HANDLED BY BRYAN CHAKOUMAKOS